

# GENERATION OF HIGH BRIGHTNESS ELECTRON BEAMS BY THE 2.4-CELL PHOTOCATHODE RF GUN\*

H. Qi, J. Wang, Z. Liu, C.-Y. Tsai, Y. Xu, K. Fan<sup>†</sup>,  
Huazhong University of Science and Technology, Wuhan, China  
J. Yang, Osaka University, Osaka, Japan

## Abstract

Modern accelerator facilities increasingly demand electron beams with improved characteristics such as shorter bunch lengths and higher brightness. To meet this demand, this study proposes a 2.4-cell photocathode electron gun, aiming to enhance the extraction electric field gradient at the cathode to produce high-quality beams. By effectively increasing this gradient, space charge effects in the low-energy region are suppressed, resulting in superior beam quality. This paper presents a detailed optimization of the gun configuration and offers a comprehensive assessment of the gun's performance through beam dynamics simulations. The simulation results demonstrate that the 2.4-cell electron gun can generate electron beams with shorter bunch lengths and lower longitudinal emittances compared to the 2.6-cell electron gun configuration.

## INTRODUCTION

The utilization of electron accelerator facilities for high-brightness light sources provides users with high-power, narrow-bandwidth radiation, fulfilling demands for material detection with superior temporal and spatial resolution. The performance of accelerator facilities, including Free Electron Lasers (FELs) [1], THz sources [2], and ultrafast electron diffraction (UED) [3], directly depends on beam quality. Consequently, the design of the electron gun, responsible for generating the electron beam supplied to the accelerator, becomes paramount.

The photocathode electron gun is noteworthy for its exceptional high acceleration gradient and relativistic output beam energy. Despite this, the brightness of the resulting beam remains substantially lower than the theoretical quantum limit expected from a fully coherent electron source, lagging by at least five orders of magnitude [4]. This presents opportunities for enhancing the gun's performance. A crucial approach for improving beam brightness involves optimizing the extraction electric field on the cathode [5]. During electron beam emission, a high-gradient electric field on the cathode can rapidly accelerate electrons away from the cathode and significantly reduce the space charge effect, thereby facilitating the generation of high-brightness electron beams.

Based on our previous research on the 1.4-cell electron gun [6], this paper presents the design of a 2.4-cell electron gun. To improve cavity quality, we employ a curved profile

and an elliptical iris connection. Additionally, we explore the potential benefits of a replaceable plug-in cathode. Through particle tracking simulations, we evaluate the performance of the gun, revealing notable improvements in longitudinal dynamics and higher brightness at pC charges.

## 2.4-CELL CAVITY DESIGN

The 2.4-cell RF photocathode electron gun is composed of two full cavities and a 0.4-cell half cavity, operating at a resonant frequency of 2856 MHz in the  $\pi$  mode. Figure 1 shows the cavity profile. The resonant frequency primarily depends on the cavity radii  $R_1$ ,  $R_2$ , and  $R_3$ . The cavity length is closely related to the flight distance of the electron over half a period, which corresponds to the length of half the wavelength of S-band. Hence, the length of the full cavity is approximately half the wavelength of the  $\pi$  mode,  $L_2 \approx 5.25$  cm, and the length of the half cavity,  $L_1 \approx 0.4L_2$ .

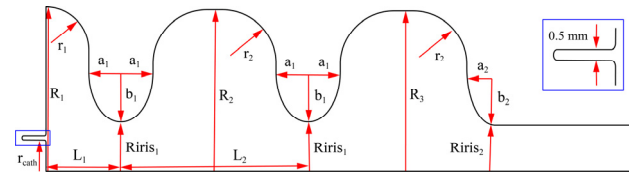


Figure 1: The 2D geometry of the 2.4-cell cavity.

To enhance the quality factor  $Q$  and achieve a more uniform distribution of the H-field on the cavity wall, we have replaced the conventional rectangular profile with a curved profile. Additionally, an elliptical iris connection has been implemented in the coupling part between each cavity. This adjustment not only reduces the presence of nonlinear electric field components but also lowers the maximal electric field on the iris surface, thereby decreasing the probability of vacuum breakdown.

The performance of an electron gun is influenced by its cavity design, which can be optimized by adjusting its parameters and considering the relationships among its physical, mathematical, and geometrical structures, ultimately aiming for a high-quality factor. To achieve this, we iteratively simulated each cavity parameter using the Superfish Poisson software [7] and validated our results through comparative analysis with CST Microwave Studio [8].

In the cavity, once the designs for both half and full cells have been finalized, the individual cells are coupled together. The cavity of the 2.4-cell electron gun contains a 3-cell geometry, which results in three modes of coupling:  $\pi$  mode,  $\pi/2$  mode, and 0 mode. Among these modes, the  $\pi$  mode is utilized for electron acceleration, whereas the  $\pi/2$  mode and the 0 mode cannot be utilized for this purpose. By precisely adjusting each cavity, the desired  $\pi$  mode can be achieved. Furthermore, the field balance is crucial as it

\* Work supported by the National Natural Science Foundation of China (NSFC 12235005), and National Key Research and Development Program of China (2022YFA1602202).

<sup>†</sup> kjfan@hust.edu.cn

varies with the coupling and cavity frequency changes. To achieve equal acceleration in each cell, a field balance of 1 is selected. The optimized geometric parameters of the resulting 2.4-cell RF gun are presented in Table 1.

Table 1: Cavity Geometry Parameters

Placement	Parameters	Value (mm)
Half-cell	$R_1$	46.2635
	$L_1$	21
	$r_1$	12
	$a_1$	9
	$b_1$	14
Mid-cell	$R_1 r_1 s_1$	14
	$R_2$	45.482
	$L_2$	52.4845
End-cell	$r_2$	15
	$R_3$	45.154
	$a_2$	8
Cathode plug	$b_2$	16
	$R_1 r_1 s_2$	13
Cathode plug	$r_{cath}$	7.5

Figure 2 shows the simulation results of electric field distribution in the cavity, using Superfish Poisson code, with the parameters outlined in Table 1. The electromagnetic field distribution is clearly identifiable as  $\pi$  mode, with a corresponding resonant frequency of 2856.02 MHz. The quality factor  $Q$  is 14057.3. The electric field contour map obtained with CST is presented in Fig. 3. The frequency of  $\pi$  mode is 2855.96 MHz, and the quality factor  $Q$  of the cavity is 14095.2. Notably, the results obtained from both Superfish Poisson and CST simulations demonstrate a high level of coherence.

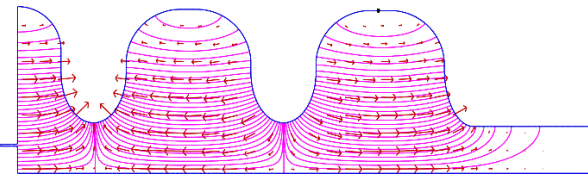
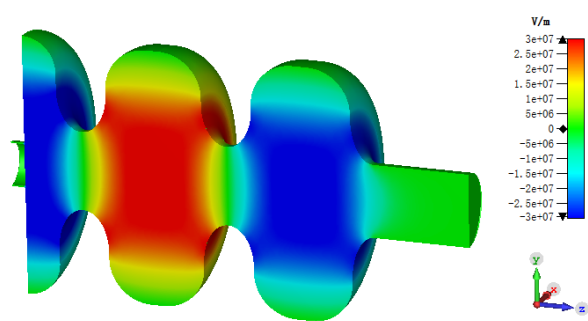
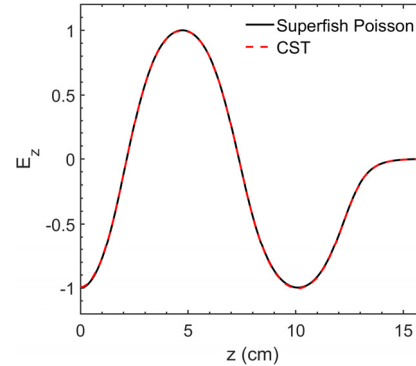


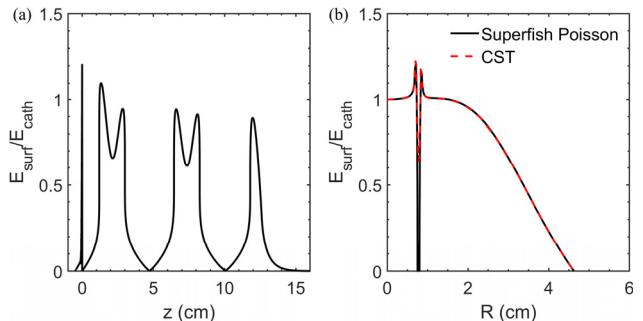
Figure 2: Electric field distribution of 2.4-cell cavity from Superfish Poisson.

Figure 3: The contour map of electric field  $E_z$  in the resonant mode from CST.

The electric field distribution along the  $z$ -axis for the cavity in  $\pi$  mode is present in Fig. 4. It can be seen that the ratio of electric field  $E_z$  in each cell remains consistent at 1:1:1. This uniform distribution of the electric field across the cells maximizes acceleration efficiency and minimizes the risk of vacuum breakdown.

Figure 4: Normalized on-axis electric field  $E_z$  along the  $z$ -direction.

It is noteworthy that a replaceable plug-in cathode is considered in the design, which ensures both the convenience of cathode material replacement and the generation of high-quality electron beams by replacing deteriorated cathodes. However, the design introduces a 0.5 mm gap between the cathode plug and the cathode plate, as shown in Fig. 1. This gap leads to charge accumulation at the gap edges and forms a local surface electric field, as shown in Fig. 5. The most pronounced surface electric field occurs near the cathode gap, potentially amplifying the surface electric field by 10%-20%. This suggests a risk of breakdown if the peak accelerating electric field exceeds 100 MV/m. Nevertheless, operating the electron gun at a peak gradient below 90 MV/m ensures safe and stable gun operation.

Figure 5: (a) The surface electric field on the cavity wall as a function of  $z$ . (b) The normalized surface field on the cathode plate as a function of radial position  $R$ .

## BEAM PERFORMANCE

In order to assess the quality of the beam produced by the 2.4-cell electron gun more accurately, we compared it to a 2.6-cell electron gun with the same profile. Utilizing the Astra software [9], we simulated the evolution of the beam in the gun. The initial injection phase  $\phi_0$  of the beam is very important for the electron gun. Electrons are able to

be accelerated at specific phase regions, whereas those outside this region will inevitably be lost.

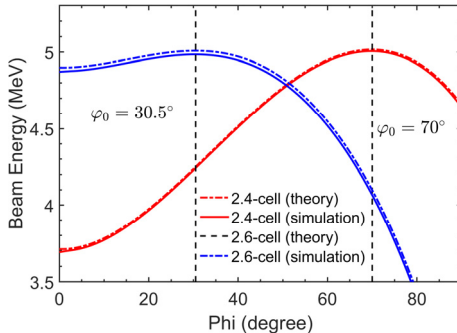


Figure 6: The beam energy of the 2.4/2.6-cell gun as a function of injection phase. The injection phases of maximum energy for the 2.4/2.6-cell gun are marked with black dashed lines.

The distribution of the electric field  $E_z(z)$  along the  $z$ -axis is expressed as:

$$E_z(z, t) = E_z(z) \sin(\omega t + \varphi_0). \quad (1)$$

Assuming the cathode serves as the starting point of the electron beam, the relationship between the  $z$ -coordinate of the beam and the flight time is given by:

$$z = c \int_0^t \beta(t') dt', \quad (2)$$

where  $\beta$  is the ratio of the velocity of the beam to the light velocity. The resulting acceleration equation for the beam is expressed as:

$$\frac{d\gamma\beta}{dt} = \frac{q}{m} E_z \left( \int_0^t \beta(t') dt' \right) \sin(\omega t + \varphi_0), \quad (3)$$

where  $q$  represents the beam charge and  $\gamma\beta$  denotes the normalized momentum of the beam. Given a specified electric field distribution  $E_z(z)$  of the electron gun, Eq. (3) can be solved numerically to obtain the beam parameters at different injection phases.

Figure 6 presents the calculated and simulated energy-injection phase curves for both the 2.4-cell and 2.6-cell electron guns, demonstrating agreement between the results. The injection phase for achieving maximum electron beam energy increases as the half-cell length decreases due to reduced travel time from the half-cell to the full cell. To achieve an electron beam of 5 MeV, the optimal phase for the 2.4-cell gun is 70 degrees, with a peak electric field gradient of 75.50 MV/m, while for the 2.6-cell gun, the optimal phase is 30.5 degrees, corresponding to a peak field gradient of 68.02 MV/m. The effective extraction electric fields on the cathode for the two electron guns are 70.95 MV/m and 34.01 MV/m, respectively, indicating a higher extraction electric field for the 2.4-cell electron gun.

To further assess the impact of varying half-cell lengths on the beam performance, we conducted simulations of electron beam distributions at the exit of two guns across a range of beam charges from 0.1 to 2 pC. In these simulations, the incident laser pulse follows a Gaussian distribution, with a spot radius of 150 mm (FWHM) and a pulse width of 100 fs (FWHM). Figure 7 shows the transverse and longitudinal emittances, bunch lengths, and brightness

of electron beams generated by the two types of guns at different beam charge states. At low beam charge states, the transverse emittance and brightness of the 2.6-cell electron gun are higher than those of the 2.4-cell gun. This is due to the weaker space charge effect at low charge levels, where the shortened half-cell enhances transverse defocusing, thereby increasing the transverse emittance induced by the RF electromagnetic field. As the charge increases, the 2.4-cell electron gun demonstrates a significant advantage in longitudinal emittance and bunch length. This superiority stems from the stronger extraction electric field of the 2.4-cell gun, which suppresses the space charge effect. Additionally, higher-brightness electron beams are produced in the 2.4-cell electron gun at pC beam charges.

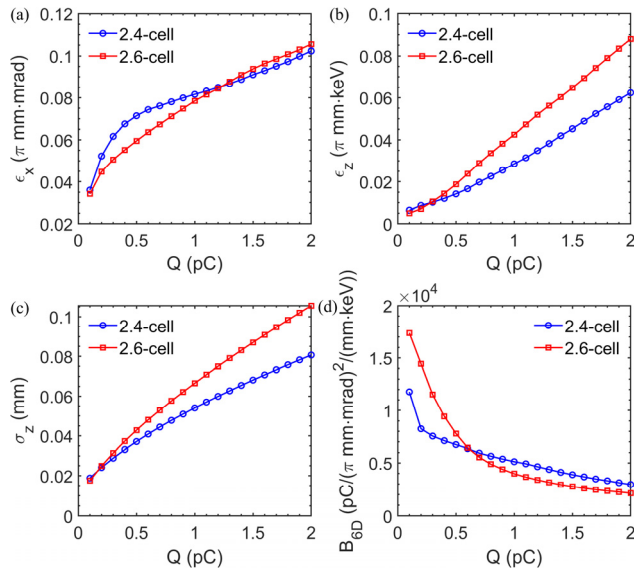


Figure 7: Comparison of beam parameters for 2.4-cell and 2.6-cell RF electron guns with varying beam charges. (a) Transverse emittance, (b) longitudinal emittance, (c) bunch length, and (d) brightness at the exit of the electron guns.

## CONCLUSION

The design of a 2.4-cell photocathode electron gun has been finalized by curving the cavity profile and incorporating elliptical iris connections in each cell. Through electromagnetic simulations, it has been demonstrated that the gun operates reliably at 2856 MHz with a field balance of 1, ensuring equal acceleration of the electron beam. Comparative analysis with a 2.6-cell electron gun of identical profile reveals notable advantages in bunch length, longitudinal emittance, and brightness for the 2.4-cell configuration. These improvements are attributed to its higher extraction electric field, which exerts a suppressive effect on the space charge effect.

## REFERENCES

[1] B. D. Patterson *et al.*, “Coherent science at the SwissFEL x-ray laser”, *New J. Phys.*, vol. 12, no. 3, p. 035012, Mar. 2010. doi:[10.1088/1367-2630/12/3/035012](https://doi.org/10.1088/1367-2630/12/3/035012)

[2] E. Chiadroni *et al.*, “A Versatile THz Source from High-Brightness Electron Beams: Generation and Characterization”, *Condens. Matter*, vol. 5, no. 2, p. 40, Apr. 2020. doi:[10.3390/condmat5020040](https://doi.org/10.3390/condmat5020040)

[3] F. Qi *et al.*, “Breaking 50 femtosecond resolution barrier in MeV ultrafast electron diffraction with a double bend achromat compressor”, *Phys Rev Lett.*, vol. 124, no. 13, p. 134803, Apr. 2020. doi:[10.1103/PhysRevLett.124.134803](https://doi.org/10.1103/PhysRevLett.124.134803)

[4] M.B. Callahan, “Quantum-Mechanical Constraints on Electron-Beam Brightness and Quality”, *IEEE J. Quant. Electron.*, vol. 24, no. 10, p. 1958, Oct. 1988. doi:[10.1109/3.8525](https://doi.org/10.1109/3.8525)

[5] E. Pirez *et al.*, “S-band 1.4 cell photoinjector design for high brightness beam generation”, *Nucl. Instrum. Methods Phys. Res. A*, vol. 865, p. 109, Sep. 2017. doi:[10.1016/j.nima.2016.08.063](https://doi.org/10.1016/j.nima.2016.08.063)

[6] Y. Song *et al.*, “Development of a 1.4-cell RF photocathode gun for single-shot MeV ultrafast electron diffraction devices with femtosecond resolution”, *Nucl. Instrum. Methods Phys. Res. A*, vol. 1031, p. 166602, May. 2022. doi:[10.1016/j.nima.2022.166602](https://doi.org/10.1016/j.nima.2022.166602)

[7] Superfish, <http://laacg.lanl.gov/laacg/services/>

[8] <http://www.cst.com>

[9] K. Floettmann, <http://www.desy.de/mpyflo/>